Carbohydrate Polymers 82 (2010) 1228–1235

Contents lists available at ScienceDirect

Carbohydrate Polymers

journal homepage: www.elsevier.com/locate/carbpol

Rheology of xanthan solutions as a function of temperature, concentration and ionic strength

Emilie Choppe, Fanny Puaud, Taco Nicolai*, Lazhar Benyahia

Polymères, Colloïdes, Interfaces (PCI), UMR CNRS 6120, Université du Maine, Avenue Oliver Messiaen, 72085 Le Mans Cedex 9, France

ARTICLE INFO

Article history:
Received 26 February 2010
Received in revised form 18 June 2010
Accepted 29 June 2010
Available online 6 July 2010

Keywords:
Xanthan
Viscosity
Gel
Rheology
Polysaccharide

ABSTRACT

The rheology of renatured xanthan solutions was studied using oscillatory and continuous shear. The effects of temperature, concentration and ionic strength were systematically investigated. These parameters mainly influence the terminal relaxation time of the solutions, while the effect on the high frequency shear modulus is relatively minor. Master curves were obtained by frequency–temperature superposition covering over 10 decades of the frequency. Frequency–concentration superposition of the master curves showed that the shear rheology of xanthan solutions is universal. The relaxation time decreases with increasing temperature and shows a transition between two states that shifts to higher temperatures with increasing ionic strength. The relaxation time increases exponentially with increasing polysaccharide concentration. The shear rate dependence of the viscosity is also described by a universal function with the same shift factors as for the oscillatory shear measurements. The master curves show a Newtonian plateau followed by strong shear thinning that can be described by a power law dependence on the shear rate. The results are interpreted in terms of the formation of a transient network of chains cross-linked by bonds with a finite lifetime.

1. Introduction

Xanthan is a bacterial polysaccharide that is much used in industrial applications as stabilizer and texturant (Born, Langendorff, Boulenguer, Steinbüchel, & Rhee, 2005; Morris, 2006; Sworn, 2000). For this reason the dynamic mechanical properties of xanthan in aqueous solution have been investigated extensively (Capron, Brigand, & Muller, 1998; Cuvelier & Launay, 1986; Lee & Brant, 2002; Oviatt & Brant, 1994; Pelletier, Viebke, Meadows, & Williams, 2001; Rochefort & Middleman, 1987; Rodd, Dunstan, & Boger, 2000; Ross-Murphy, Morris, & Morris, 1983; Whitcomb & Macosko, 1978; Wyatt & Liberatore, 2009). For a given temperature the viscosity increases strongly with increasing concentration, while it decreases strongly with increasing temperature especially at low ionic strength. The strong temperature dependence is attributed to a conformational transition of xanthan chains from helical at low temperatures to random coil at high temperatures (Paoletti, Cesaro, & Delben, 1983). The characteristic temperature of this transition increases with increasing ionic strength and was found to be the same when determined using rheology or techniques that probe more directly the molecular conformation such as optical rotation.

Upon cooling the xanthan returns to the helical conformation, but does not fully recover its native state. For this reason a distinction is made between native and renatured xanthan (Capron et al., 1998; Matsuda, Biyajima, & Sato, 2009). Commercial samples are often partially renatured and their properties depend on further heat treatment. However, if the heat treatment is sufficient so that all xanthan is denatured the system is no longer sensitive to the thermal history. For the investigation presented here we made sure that the rheology no longer depended on the thermal history of xanthan.

At lower temperatures and higher concentrations the solutions behave like gels characterized by a storage shear modulus (G') larger than the loss modulus (G''). Both are only weakly dependent on the oscillation frequency in the accessible range. In order to extend the dynamic range it is common practice to do measurements as a function of the temperature and to create master curves by frequency–temperature superposition. This was done by a few research groups for xanthan solutions. Rochefort and Middleman (1987) reported that good superposition was obtained in the presence of 86 mM NaCl, while without added salt the superposition was not so good. They explained this by the helix–coil transition that occurred in the salt free solutions within the temperature range covered in the experiment. More recently, Pelletier et al. (2001) studied xanthan solutions at 100 and 8.6 mM NaCl. They found that in both cases good superposition was obtained even though the transition occurred within the temperature range covered in the experiment.

* Corresponding author.
E-mail address: Taco.Nicolai@univ-lemans.fr (T. Nicolai).

0144-8617/$ – see front matter © 2010 Elsevier Ltd. All rights reserved.
doi:10.1016/j.carbpol.2010.06.056

An alternative method to extend the dynamic range is to measure different concentrations at a fixed temperature and create master curves by frequency–concentration superposition. Cuvelier and Launay (1986) found good superposition for concentrations between 2 and 8 g/L and for concentrations between 0.25 and 1.25 g/L, but the master curves thus obtained were not the same. On the other hand, Milas, Rinaudo, Knipper, and Schuppiser (1990) and Oviatt and Brant (1993) found good superposition for the whole range between 0.16 and 3 g/L and between 10 and 30 g/L, respectively. All these measurements were done at 100 mM NaCl. A third method consisting of varying the visco-elastic properties of xanthan solutions by varying the ionic strength has not yet been investigated.

If both frequency–temperature and frequency–concentration superposition are successful, then the two methods can in principle be combined to obtain a single master curve. This has been done, for example, by Chronakis, Doublier, and Piculell (2000) for kappa-carrageenan. As far as we are aware, it has not yet been attempted for xanthan solutions. The combination of varying both parameters allows one to test more comprehensively whether the relaxation process of xanthan in solution is universal.

Here we present an extensive investigation of xanthan solutions over a range of concentrations (2–20 g/L), temperatures (5–90 °C) and NaCl concentrations (0–100 mM) using oscillatory shear. We will show that a single master curve can describe all xanthan solutions. We have also calculated the corresponding dynamic viscosity and compared it with the measured shear rate dependent viscosity. Three different commercial batches of xanthan were found to yield the same master curve, although the shift factors were batch dependent. The consequences of our observations for possible molecular models of semi-dilute xanthan solutions are discussed.

2. Experimental

2.1. Materials

Most of the experiments were done using the xanthan sample RH200 obtained from Rhodia. Two other samples were investigated more succinctly in order to test the generality of the results: RH80 from Rhodia (France) and CX91 from Cargill (France).

The intrinsic viscosities were determined at 25 °C: 1.17 L/g for RH200; 1.34 L/g for RH80; 1.59 L/g for CX91, but the true values could be higher because of non-Newtonian behaviour persisting to low concentrations. Little difference was found for systems in 0.1 M NaCl and without added salt. Analysis of the mineral content showed that the counterion was sodium and that the powders contained trace amounts of calcium and potassium ions (<0.05%, w/w). The powders were dissolved in ultrapure water (Millipore) to which 3 mM NaN_3 was added as a bacteriostatic agent. The pH of the solutions was 6.8 unless otherwise specified. The NaCl concentration was set by adding required amounts of a concentrated NaCl solution. In some trials the solutions were dialysed, but we did not find a significant effect of dialysis on the results.

2.2. Rheology

Oscillatory and continuous shear experiments were done using a stress imposed rheometer with a Couette geometry: MCR 301, Physica, Anton Paar or AR2000, TA Instruments. In both cases the gap was 1 mm and the radius was close to 30 mm. The imposed stress during oscillatory shear measurements was chosen within the linear response regime. At each temperature the system was left to equilibrate for 15 min before starting the measurement. We checked that this waiting period was enough to reach steady state. The intrinsic viscosity was determined by measuring the viscosities of xanthan solutions using an Ubbelohde viscometer between 0.01 and 0.1 g/L.

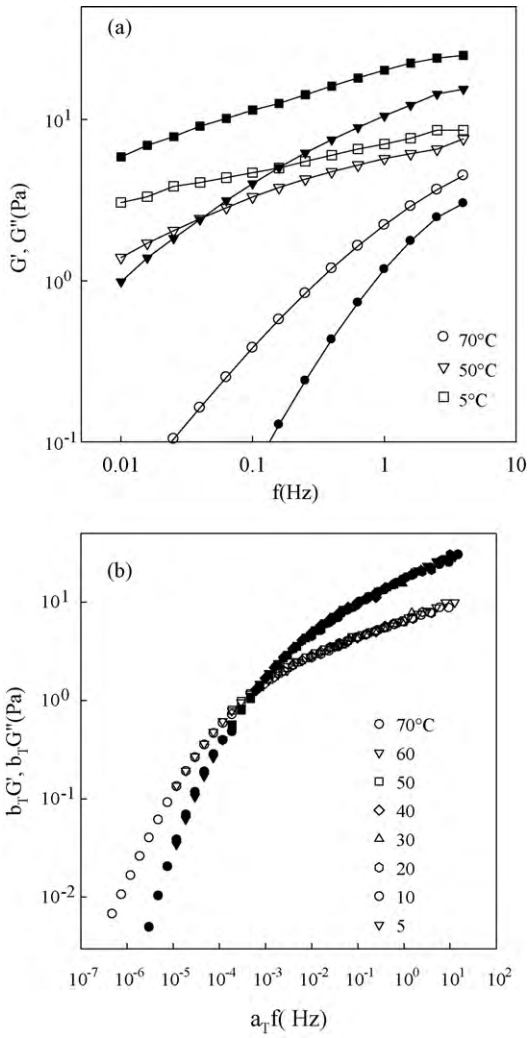

Fig. 1. (a) Frequency dependence of the storage (filled symbols) and the loss (open symbols) modulus of a xanthan solution with $C = 10$ g/L without added salt at 3 temperatures as indicated in the figure. (b) Master curves of the frequency dependence of the storage (filled symbols) and the loss (open symbols) modulus of a xanthan solution with $C = 10$ g/L without added salt at a range of temperatures obtained by horizontal and vertical shifts. The reference temperature is 20 °C.

3. Results

Preliminary measurements of the shear modulus as a function of the temperature showed that the results during the first heating and cooling ramps between 0 and 90 °C were different from subsequent ramps. This effect was studied in more detail by Capron et al. (1998) and was attributed to heat induced denaturation of native xanthan. Denatured xanthan renatures again upon cooling, but the structure of renatured xanthan is different from that of native xanthan. In order to avoid any ambiguity about the state of the xanthan in solution we have preheated all solutions and made sure that the results became independent of further heat treatment. This means that we studied renatured xanthan. We also noted an effect of the heating and cooling rate on the temperature dependence of the shear moduli. Therefore we have studied the systems at fixed temperatures after stabilization, which could take up to 10 min.

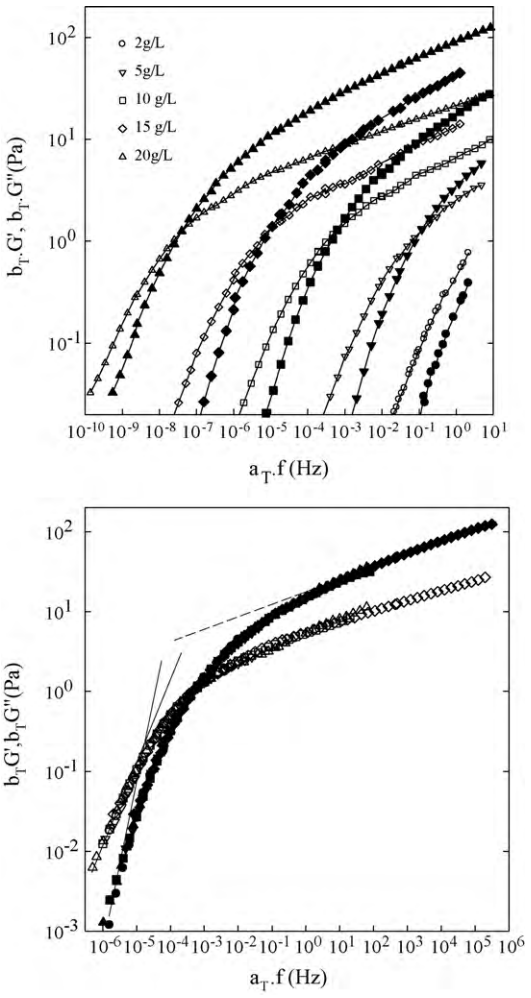

Fig. 2. (a) Master curves of the frequency dependence of the storage (filled symbols) and the loss (open symbols) modulus of xanthan solution with different concentrations without added salt. The master curves of all concentrations were obtained by time–temperature superposition as in Fig. 1b, but for clarity not all data points are shown. The reference temperature is 20 °C in each case. (b) Master curves of the data shown in (a) obtained by horizontal and vertical shifts with respect to the system at 10 g/L. The solid lines represent the frequency dependences for Newtonian liquids. The dashed line has slope 0.16.

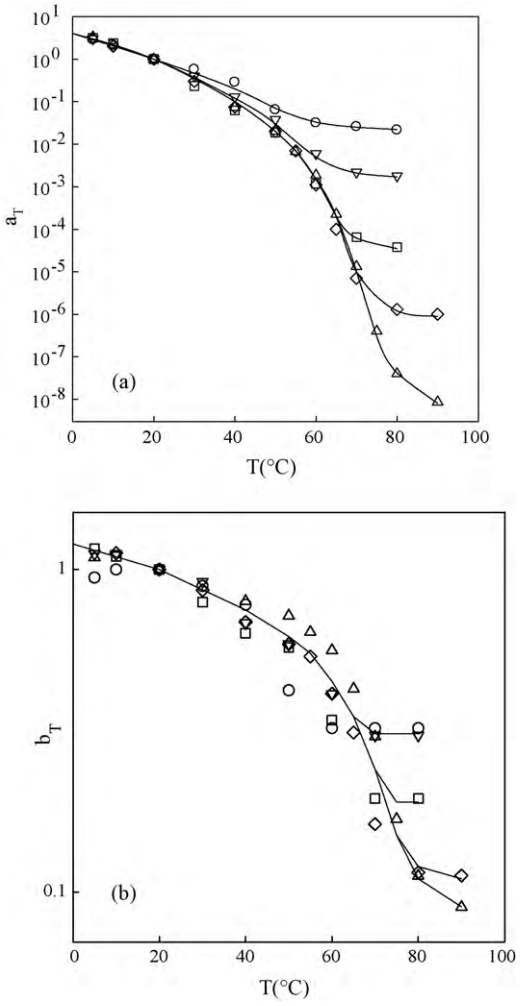

Fig. 3. Horizontal (a) and vertical (b) shift factors used to obtain the master curves shown in Fig. 2a. Symbols as in Fig. 2a. The solid lines represent guides to the eye.

Fig. 1a shows examples of the frequency dependence of G' and G'' for a xanthan solution without added salt at $C = 10$ g/L. At 70 °C the system behaves liquid-like over most of the frequency range covered in the experiment. At 50 °C, G' crosses G'' at $f = 0.03$ Hz, while at 5 °C the system behaves solid-like over the whole frequency range. Master curves of G' and G'' could be obtained using horizontal and vertical shifts. The results with reference temperature $T_{ref} = 20$ °C are plotted in Fig. 1b and show that frequency–temperature superposition is very good for this system over the whole temperature range. The frequency dependence shows that the xanthan solution is visco-elastic with a liquid-like behaviour at low frequencies and tends to a solid-like behaviour at high frequencies.

The same procedure was followed for solutions with different xanthan concentrations between 2 and 20 g/L. At lower concentrations the moduli were too weak even at 5 °C to obtain accurate results. Master curves at $T_{ref} = 20$ °C are plotted in Fig. 2a. In each case excellent frequency–temperature superposition was obtained over the whole temperature range. The horizontal (a_T) and vertical (b_T) shift factors used in the frequency–temperature superposition are plotted in Fig. 3a and b, respectively. a_T represents the variation of the relaxation times, while b_T represents the variation of the amplitude of the elastic modulus. We note that, while at higher temperatures the shift parameters can be obtained with good precision, the superposition is more ambiguous at lower temperatures where the frequency dependence of G' and G'' is small.

The temperature dependence of a_T covers many orders of magnitude, while b_T varied by at most a factor of 10. At each concentration both a_T and b_T have a sigmoidal temperature dependence. With increasing temperature a_T decreases weakly at first followed by a steep decrease starting at about 40 °C. This behaviour is indicated by the solid lines and does not depend on the concentration in a systematic manner. At higher temperatures the shift factors appear to stabilize at a value that decreases with decreasing concentration. The total variation of a_T increases with increasing concentration from about 2 decades at 2 g/L to more than 8 decades at 20 g/L.

The shape of the master curves is the same, but the cross-over of G' and G'' shifts to lower frequencies with increasing concentration. A single master curve could be obtained using horizontal and vertical shifts. The result is plotted in Fig. 2b at $C_{ref} = 10$ g/L and shows that frequency–concentration superposition was excellent in the concentration range covered here. The solid lines show that the purely liquid response is reached at the lowest frequencies ($G' \propto \omega^2$; $G'' \propto \omega$). The dashed line indicates that G' has a weak power law dependence at high frequencies ($G' \propto \omega^{0.16}$).

The horizontal shift factors (a_C) used in the frequency–concentration superposition are plotted in Fig. 4.

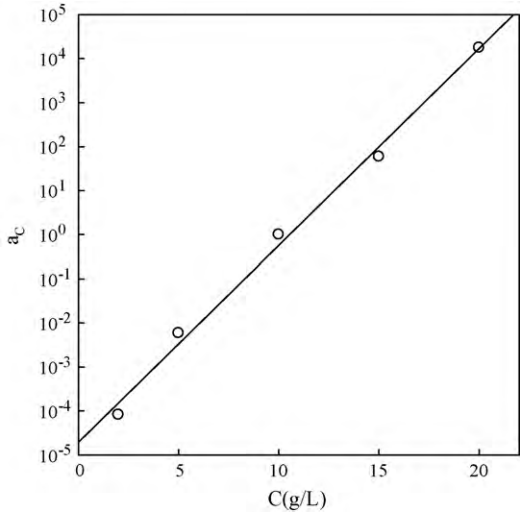

Fig. 4. Horizontal shift factors used to obtain the master curves shown in Fig. 2b.

They show a large increase between 2 and 20 g/L that can be well described by an exponential: $a_C = 2.5 \times 10^{-5}$ exp(0.97C) with C in g/L. The vertical shift factors are close to unity over the whole range, as can be easily seen from the weak variation of the values of G' and G'' at the cross-over, see Fig. 2a.

The effect of the ionic strength was investigated at $C = 10$ g/L by varying the added NaCl concentration up to $C_s = 100$ mM. Again excellent frequency–temperature was obtained at each ionic strength. Fig. 5a compares master curves with $T_{ref} = 20\,^{\circ}$C obtained at different NaCl concentrations. The master curve obtained at $C_s = 10$ mM was indistinguishable from that without added NaCl. Notice that all solutions contained 3 mM NaN_3 in addition to the added NaCl. With increasing ionic strength the cross-over between G' and G'' shifts to lower frequencies and slightly lower moduli. The horizontal shift factors used to obtain the master curves are plotted in Fig. 5b. Both at low and very high temperatures the shift factors are independent of the ionic strength. There is a steep transition between the two regimes that occurs at higher temperatures as the salt concentration is raised and is not visible for $C_s = 100$ mM up to 90 °C. The vertical shift factors show the same features, but not as clearly because their variation is much smaller.

The master curves at different ionic strengths superimpose well unto the results obtained in the absence of added NaCl, see Fig. 6. The resulting master curve is, of course, the same as the one obtained from the frequency–concentration shifts shown in Fig. 2b since the data without added NaCl are common. The horizontal shift factors (a_s) used in the frequency–ionic strength superposition are 3.7 at 20 mM, 200 at 50 mM and 400 at 100 mM. The vertical shift factors (b_s) are close to unity: 1.1, 1.5 and 1.5 at 20, 50 and 100 mM, respectively. The effect of adding salt at a given concentration is important, but much smaller than the effect of varying the xanthan concentration.

We also investigated the flow behaviour of the xanthan solutions. In Fig. 7 the viscosity is plotted as a function of the shear rate for $C = 15$ g/L without added salt at a few chosen temperatures. We checked that steady state was obtained at each shear rate. No difference was found when the shear rate was progressively increased or decreased. The results are compared with the dynamic viscosity plotted as a function of the radial frequency (ω). As was reported before by others, the viscosity strongly decreases above a critical shear rate that decreases with increasing concentration. It appears that at high shear rates the viscosity becomes almost independent of the temperature. The viscosity was equal to the dynamic viscosity at high temperatures where the effect of shear thinning was

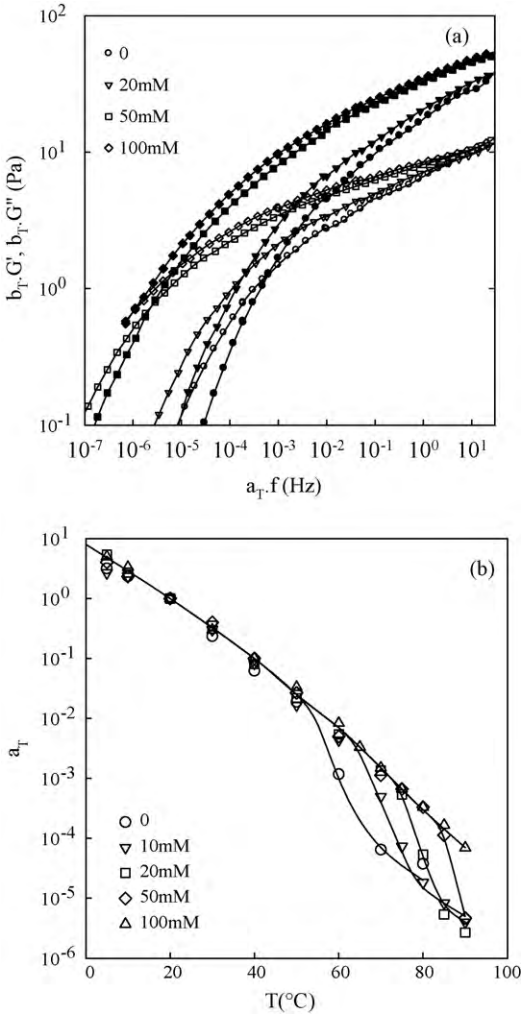

Fig. 5. (a) Master curves of the frequency dependence of the storage (filled symbols) and the loss (open symbols) modulus of xanthan solution with $C = 10$ g/L at different NaCl concentrations indicated in the figure. The master curves at each ionic strength were obtained by frequency–temperature superposition as in Fig. 1b, but for clarity not all data points are shown. The reference temperature is 20 °C in each case. (b) Horizontal shift factors used to obtain the master curves at different ionic strengths indicated in the figure. The solid lines represent guides to the eye.

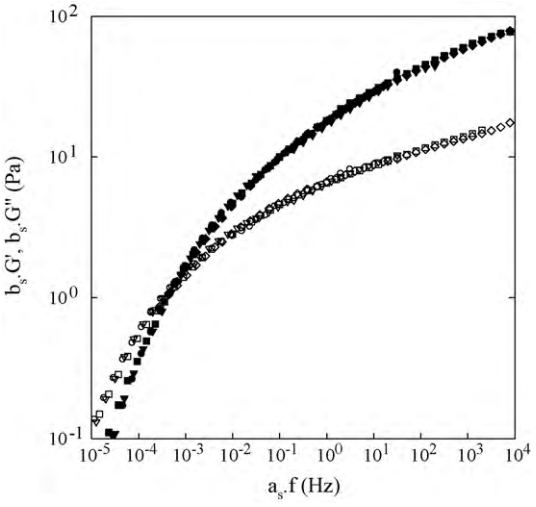

Fig. 6. Master curves of the data shown in Fig. 5a obtained by horizontal and vertical shifts with respect to the system without added salt. Symbols as in Fig. 5a.

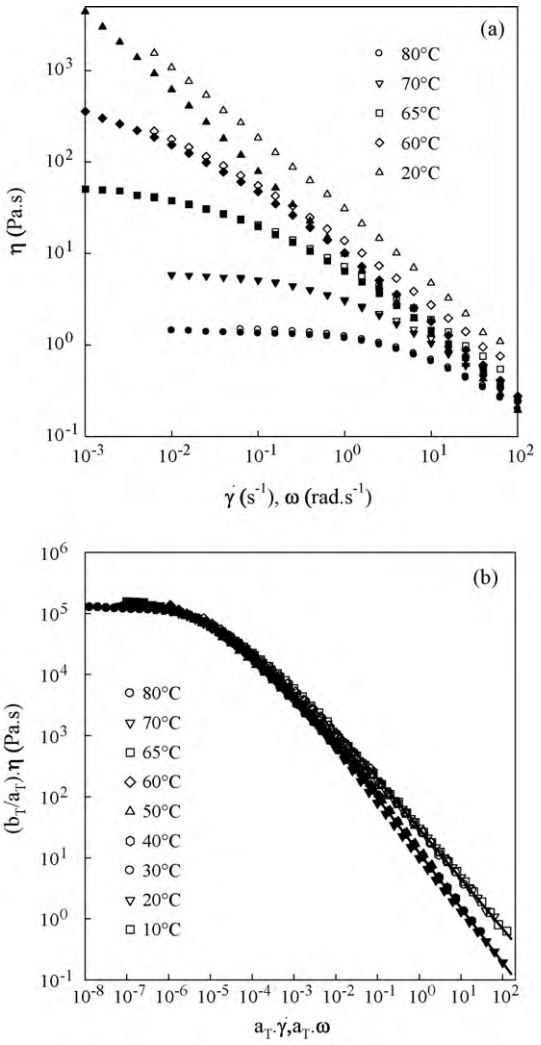

Fig. 7. (a) Comparison of the shear rate dependent viscosity (closed symbols) with the dynamic viscosity (open symbols) calculated from G' and G'' for a xanthan solution at $C = 15$ g/L without added salt at different temperatures. (b) Master curves of the viscosity and the dynamic viscosity obtained by vertical and horizontal shifts with $T_{ref} = 20\,^{\circ}C$. The solid lines through the results of the viscosity and the dynamic viscosity at high frequencies have slopes −0.90 and −0.84, respectively.

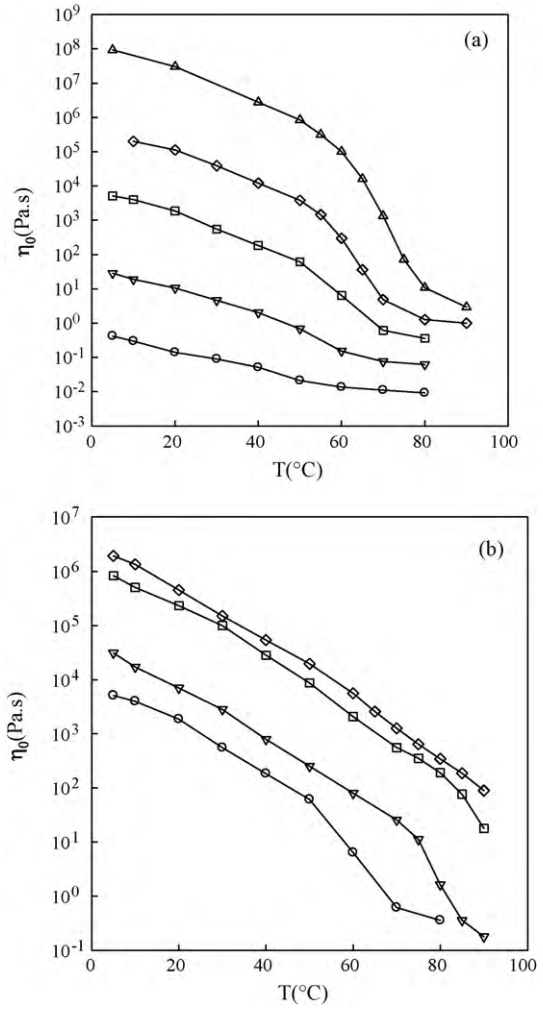

Fig. 8. Temperature dependence of the low-shear viscosity of xanthan solutions at 20 °C for different concentrations without added NaCl (Fig. 8a) and for different ionic strengths at $C = 10$ g/L (b). Symbols as in Figs. 2a and 5a.

relatively small. However, at low temperatures we found that the viscosity was smaller than the dynamic viscosity implying that the so-called Cox–Merz rule is not obeyed for this system.

Master curves of the shear rate dependent viscosity could be obtained using frequency–temperature superposition with the same shift factors that were used for the oscillatory measurements. The master curves show clearly that the difference between the viscosity and the dynamic viscosity increases with increasing shear rate and is only obvious deep in the shear thinning regime. Larger dynamic viscosity in the strongly shear thinning regime was reported earlier (Lee & Brant, 2002; Oviatt & Brant, 1994; Pelletier et al., 2001; Ross-Murphy et al., 1983). On the other hand Wyatt and Liberatore (2009) found that the Cox–Merz rule was observed for xanthan solutions, but the solutions that they studied were not strongly shear thinning.

The dependence of the viscosity on the shear rate at high shear rates can be approximated by a power law at least up to 100 s^{-1}. The slopes are −0.90 for the viscosity and −0.84 for the dynamic viscosity. The latter is, of course, directly related to the high frequency dependence of G'. The same behaviour was found at other xanthan concentrations and also if salt was added. The implication is that xanthan solutions flow with less stress at higher shear rates than expected on the basis of the frequency dependent shear moduli in the linear response regime. The shear rate–temperature superposition allows us to deduce the limiting low-shear viscosity at temperatures and concentrations where direct measurements are not possible. For example Fig. 7 shows that the low-shear viscosity at $C = 15$ g/L and 20 °C is more than 10^5 Pa s^{-1}. The low-shear viscosity of this system could only be determined directly using flow rates less than 10^{-5} s^{-1}. Obviously, such systems are indistinguishable from permanently bound gels.

The low-shear viscosities (η_0) of xanthan solutions at all temperatures, concentrations and ionic strengths studied here can be derived from the shift factors shown in Figs. 3 and 5b. As an example we show the temperature dependence of the low-shear viscosity of xanthan solutions at 20 °C for different concentrations without added NaCl (Fig. 8a) and for different ionic strengths at $C = 10$ g/L (Fig. 8b). In Fig. 9 we show the concentration dependence in the absence of added salt at two temperatures 20 and 80 °C. As mentioned above, the shear modulus is independent of the concentration at least between 2 and 20 g/L. Therefore the viscosity varies in the same way as the terminal relaxation time, which was already shown for $T_{ref} = 20\,^{\circ}C$ in Fig. 4. In Fig. 9 we included values of the viscosity at lower concentrations for which G' could not be measured. As might be expected, the concentration dependence below 2 g/L deviates from the exponential dependence observed for semi-dilute xanthan solutions towards the solvent viscosity.

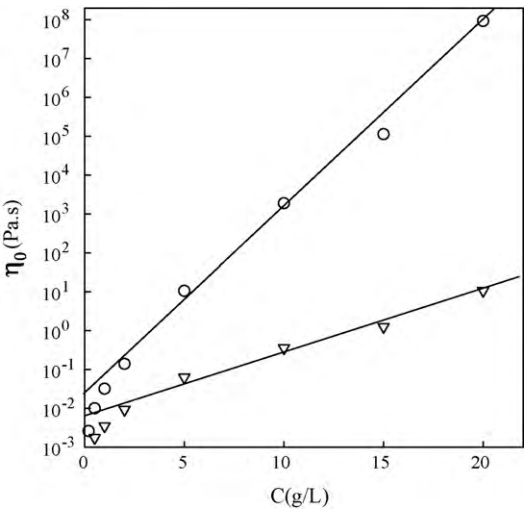

Fig. 9. Semi-logarithmic representation of the concentration dependence of the low-shear viscosity without added salt at 20 °C (circles) and at 80 °C (triangles). The solid lines represent exponential concentration dependence.

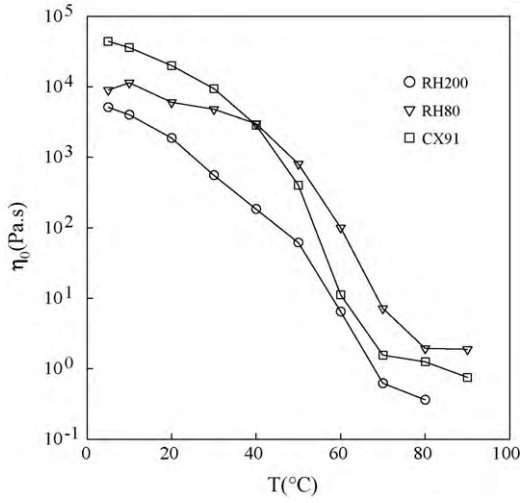

Fig. 10. Temperature dependence of the low-shear viscosity of solutions prepared from different xanthan samples at 20 °C, C = 10 g/L, without added NaCl.

The viscosity at 80 °C is much lower, but still shows an exponential concentration dependence for $C > 2$ g/L.

We also looked at the effect of the pH between 5.5 and 8.5, but we did not find a significant influence of the pH on the rheology, as might be expected from the weak variation of the charge density of xanthan in this range (Bezemer, Ubbink, Dekooker, Kuil, & Leyte, 1993). Furthermore, we investigated two other xanthan samples at a few concentrations and ionic strengths in order to test the generality of the results. Identical master curves were obtained, but the absolute values of shear moduli and the viscosities were different. In Fig. 10 the temperature dependence of the viscosity at C = 10 g/L without added NaCl is compared. The transition temperatures are close, but the shift factors are somewhat different which is possibly caused by a modification structure of the xanthan chain, but we did not investigate this issue in more detail for this study. The variation between the different samples is small compared to the huge dependence on the concentration.

4. Discussion

Before discussing possible molecular models of xanthan solutions, let us first summarise the main observations presented here. The frequency dependence of the shear moduli is universal for aqueous xanthan solutions independent of the temperature (5–90 °C), concentration (3–20 g/L) and ionic strength (3–100 mM) at least in the range investigated. The relaxation is characterized by a broad distribution of relaxation times covering many decades. Perhaps surprisingly, the conformational transition did not have a significant effect on the frequency dependence of G' and G''. The important implication is that the relaxation mechanism of xanthan solutions is the same in both conformations.

The terminal relaxation time decreased approximately exponentially with increasing temperature in the helix conformation, see Fig. 5b. It also appears to decrease in the coil conformation, but this state could only be studied over a small range of high temperatures. The transition itself had the additional effect of strongly speeding up the relaxation, especially at higher concentrations. The amplitude of the shear moduli increased with increasing temperature and also showed a strong effect of the transition at higher concentrations. However, the variation of the relaxation times was much larger and therefore was the main cause of the temperature dependence of the viscosity.

The terminal relaxation time increased approximately exponentially with increasing xanthan concentration, but the amplitude of the shear moduli varied only very little. The effect of the ionic strength on the terminal relaxation time was smaller, but still it increased by more than two orders of magnitude when 100 mM NaCl was added at lower temperatures, i.e. when xanthan is in the helix conformation. The effect of adding salt was much larger at high temperatures where it led to a conformational transition. The transition temperature increased by about 40 °C after 100 mM NaCl was added. The increase of the transition temperature with increasing ionic strength was already reported and discussed in detail by Paoletti et al. (1983). We noted almost no effect of the ionic strength on the amplitude of the shear moduli.

These observations complement and extend those reported in the literature. As was mentioned in the introduction, frequency–temperature superposition was attempted earlier for xanthan solutions. Rochefort and Middleman (1987) studied the frequency dependence of G' and G'' as a function of the temperature for C = 5 g/L. The results obtained on a different commercial xanthan sample are close to the one obtained in our study. Good superposition was obtained in the presence of 86 mM NaCl, but in distilled water superposition was not successful. The latter result contradicts our observation that good superposition is possible also at low ionic strengths. However, they assumed that the vertical shift factors were simply proportional to the absolute temperature as would be the case for pure rubber elasticity. It is likely that much better superposition would have been obtained if they had allowed a different temperature dependence of b_T.

Pelletier et al. (2001) studied xanthan solutions at C = 10 g/L and 8 mM NaCl. They found good frequency–temperature superposition for G' even though they fixed b_T at unity. Most likely, better superposition also for G'' would have been found if b_T had been allowed to vary. The superposition was obtained over a temperature range within which dynamic scanning calorimetry showed that a conformational transition occurred at about 50 °C. These results are in agreement with our finding that the transition does not lead to a significantly different frequency dependence of the shear moduli. The authors interpreted the temperature dependence of a_T in terms of the so-called Williams, Landau, Ferry equation that is successfully used for polymer melts near the glass transition temperature. However, there is no reason to suppose that glass transition dynamics are relevant for semi-dilute xanthan solutions.

Frequency–concentration superposition at fixed temperatures was attempted in three previous investigations. In all cases the temperature was fixed at 25 °C and the xanthan solutions con-

tained 100 mM NaCl. Cuvelier and Launay (1986) found good superposition between 2 and 8 g/L using horizontal shift factors that increased with increasing concentration following a power law and vertical shift factors that remained close to unity. These results are fully compatible with our findings based on frequency–concentration superposition of master curves obtained from frequency–temperature superposition and therefore with a much broader dynamical range. However, by extending to higher concentrations we find that a_C is better described by an exponential rather than a steep power law. In the lower concentration range between 0.16 and 1.25 g/L they found that superposition led to a different master curve using horizontal shift factors that decreased weakly with increasing concentration ($a_C \propto C^{-1}$), but with a rather strong dependence of b_c ($b_c \propto C^{-2.9}$). Milas et al. (1990) obtained a single master curve in the range 0.16–3 g/L by superimposing the shear moduli normalized by the concentration, i.e. forcing $b_c \propto C^{-1}$, and using horizontal shift factors that increased with increasing concentration. Oviatt and Brant (1993) obtained a master curve for xanthan at 100 mM NaCl at higher concentrations between 10 and 30 g/L using horizontal shifts and forcing $b_c \propto C^{-1}$. The reason for choosing $b_c \propto C^{-1}$ is that the number of Rouse modes is proportional to the concentration, but this choice is justified only if the origin of the shear modulus is entropic and caused by deformation of flexible, unentangled polymers. There are good reasons to suppose that this is not the case for semi-dilute xanthan solutions, see below.

Recently, Song, Kim, and Chang (2006) reported flow measurements on xanthan solutions between 10 and 40 g/L at 20 °C. The experimental results resemble those reported here for xanthan at higher concentrations and lower temperatures. They also found that the viscosity decreased with increasing shear rate following approximately a power law. However, they concluded that the solutions had a yield stress. Marcotte, Taherian Hoshahili, and Ramaswamy (2001) came to the same conclusion for xanthan at 10 g/L measured at 20 °C. The present results show that this conclusion may be erroneous and that an apparent yield stress is observed only when the system is studied over a limited dynamical range.

The results shown here render highly unlikely the possibility that in the concentration range studied here xanthan solutions are entangled polymer solutions without specific attractive interactions as was suggested by Milas et al. (1990) and more recently by Wyatt and Liberatore (2009). The concentration dependence of the terminal relaxation time of such systems is expected to be much smaller, while the concentration dependence of the shear moduli is expected to be much larger. In addition, the temperature dependence of the terminal relaxation time is much too large even if we do not consider the coil–helix transition.

Another possibility is that xanthan chains form a transient network of chains cross-linked by bonds with a finite lifetime (Lim, Uhl, & Prudhomme, 1984; Oviatt & Brant, 1993; Rochefort & Middleman, 1987; Ross-Murphy et al., 1983). If the chains are flexible between the cross-links the storage shear modulus can be estimated using the theory of rubber elasticity (Mark, Erman, & Bokobza, 2007):

$$G' = a\nu kT \quad (1)$$

where ν is the number concentration of elastically active chains, kT is the thermal energy and a is a constant of order unity. The deformation of the xanthan chains and thus G' relaxes only if transient cross-links break. Many observed features can be explained by this model. The broad relaxation time distribution would suggest a broad distribution of bonding energies and thus of bond life times. The temperature dependence of the terminal relaxation time can be explained by an increase of the bond energy with decreasing temperature for xanthan chains in either the helix or the coil conformation. The sharp variation of G' and the terminal relaxation time at the transition would indicate that in the helix conformation fewer transient bonds are formed, but they have a larger bond energy. Screening the electrostatic interactions by adding salt could also increase the bond energy without changing significantly the number of cross-links.

More difficult to explain with this model is the observed concentration dependence. For a network of associating flexible chains one expects that the number of cross-links and thus G' increases approximately with the square of the polymer concentration. Notice that such concentration dependence is also expected for entangled polymers. Here we find almost no variation of G' with the concentration. A further argument that the elasticity is most likely not caused by rubber elasticity is that the distance between elastically active cross-links ($\xi = \nu^{-1/3}$) calculated using Eq. (1) is between about 30 and 70 nm for G' between 10 and 100 Pa, which is less than the estimated persistence length of xanthan (Berth et al., 1996; Camesano & Wilkinson, 2001; Capron, Brigand, & Muller, 1997; Coviello, Kajiwara, Burchard, Dentini, & Crescenzi, 1986; Sato, Norisuye, & Fujita, 1984). Small angle neutron scattering experiments showed that the local structure of the network resembles that of hexagonally packed rigid rods (Milas, Rinaudo, Duplessix, Borsali, & Lindner, 1995).

It appears that the network is formed by a relatively low concentration of the chains and that additional chains increase the lifetime of the existing cross-links, but do not contribute to the elasticity. Cuvelier and Launay (1986) arrived at the same conclusion and suggested that parallel packing of the semi-rigid xanthan chains causes this peculiar behaviour that has, as far as we know, not been observed for other transiently cross-linked polymer solutions. The network is easily perturbed by flow, but reforms relatively quickly after cessation of the flow.

5. Conclusion

The shear modulus and the shear rate dependence of the viscosity of xanthan solutions is a universal function of the frequency normalized by a characteristic relaxation time at temperatures between 5 and 90 °C, concentrations between 2 and 20 g/L and Na^+ concentrations between 3 and 100 mM. The relaxation time increases exponentially with increasing concentration. It decreases with increasing temperature following a sigmoidal shape. The temperature of the steepest decrease increases with increasing ionic strength. At all temperatures the relaxation time increases with increasing ionic strength. The shear modulus increases with increasing temperature, but is almost independent of the xanthan and the salt concentration.

The shear rate dependence of the viscosity is also described by a universal master curve with the same shift factors as for the oscillatory shear measurements. Xanthan solutions show strong shear thinning that can be described by a power law dependence of the viscosity on the shear rate. The viscosity is close to the dynamic viscosity calculated from oscillatory measurements, but systematically smaller deep in the shear thinning regime.

Different commercial xanthan samples can be described by the same universal behaviour, but the relaxation times depend on the sample.

The results show that semi-dilute xanthan solutions are not non-interacting entangled polymer solutions. More likely xanthan forms a transient network of chains cross-linked by bonds with a finite lifetime. The strength of the transient gel is only weakly dependent on the xanthan concentration and the ionic strength, but the lifetime of the bonds is strongly dependent on these parameters. The coil–helix transition decreases the gel strength but, more importantly, it increases the bond lifetime, especially at higher xanthan concentrations.

References

Berth, G., Dautzenberg, H., Christensen, B. E., Harding, S. E., Rother, G., & Smidsrod, O. (1996). Static light scattering studies on xanthan in aqueous solutions. *Macromolecules*, *29*(10), 3491–3498.

Bezemer, L., Ubbink, J. B., Dekooker, J. A., Kuil, M. E., & Leyte, J. C. (1993). On the conformational transitions of native xanthan. *Macromolecules*, *26*(24), 6436–6446.

Born, K., Langendorff, V., Boulenguer, P., Steinbüchel, A., & Rhee, S. K. (2005). Xanthan. In A. Steinbüchel, & S. K. Rhee (Eds.), *Polysaccharides and polyamides in the food industry: Properties, production, and patents* (pp. 481–519). Weinheim: Wiley–VCH.

Camesano, T. A., & Wilkinson, K. J. (2001). Single molecule study of xanthan conformation using atomic force microscopy. *Biomacromolecules*, *2*(4), 1184–1191.

Capron, I., Brigand, G., & Muller, G. (1997). About the native and renatured conformation of xanthan exopolysaccharide. *Polymer*, *38*(21), 5289–5295.

Capron, I., Brigand, G., & Muller, G. (1998). Thermal denaturation and renaturation of a fermentation broth of xanthan: Rheological consequences. *International Journal of Biological Macromolecules*, *23*(3), 215–225.

Chronakis, I. S., Doublier, J. L., & Piculell, L. (2000). Viscoelastic properties for kappa- and iota-carrageenan in aqueous NaI from the liquid-like to the solid-like behaviour. *International Journal of Biological Macromolecules*, *28*(1), 1–14.

Coviello, T., Kajiwara, K., Burchard, W., Dentini, M., & Crescenzi, V. (1986). Solution properties of xanthan. 1. Dynamic and static light-scattering from native and modifies xanthans in dilute-solutions. *Macromolecules*, *19*(11), 2826–2831.

Cuvelier, G., & Launay, B. (1986). Concentration regimes in xanthan gum solutions deduced from flow and viscoelastic properties. *Carbohydrate Polymers*, *6*(5), 321–333.

Lee, H. C., & Brant, D. A. (2002). Rheology of concentrated isotropic and anisotropic xanthan solutions. 2. A semiflexible wormlike intermediate molecular weight sample. *Macromolecules*, *35*(6), 2223–2234.

Lim, T., Uhl, J. T., & Prudhomme, R. K. (1984). Rheology of self-associating concentrated xanthan solutions. *Journal of Rheology*, *28*(4), 367–379.

Marcotte, M., Taherian Hoshahili, A. R., & Ramaswamy, H. S. (2001). Rheological properties of selected hydrocolloids as a function of concentration and temperature. *Food Research International*, *34*(8), 695–703.

Mark, J. E., Erman, B., & Bokobza, L. (2007). *Rubberlike elasticity: A molecular primer*. Cambridge University Press.

Matsuda, Y., Biyajima, Y., & Sato, T. (2009). Thermal denaturation, renaturation, and aggregation of a double-helical polysaccharide xanthan in aqueous solution. *Polymer Journal*, *41*, 526–532.

Milas, M., Rinaudo, M., Duplessix, R., Borsali, R., & Lindner, P. (1995). Small-angle neutron-scattering from polyelectrolyte solutions – From disordered to ordered xanthan chain conformation. *Macromolecules*, *28*(9), 3119–3124.

Milas, M., Rinaudo, M., Knipper, M., & Schuppiser, J. L. (1990). Flow and viscoelastic properties of xanthan gum solutions. *Macromolecules*, *23*(9), 2506–2511.

Morris, E. R. (2006). Bacterial polysaccharides. In A. M. Stephen, G. O. Philips, & P. A. Williams (Eds.), *Food polysaccharides and their applications* (p. 239). Boca Raton: CRC Press.

Oviatt, H. W., & Brant, D. A. (1993). Thermal treatment of semi-dilute aqueous xanthan solutions yields weak gels with properties resembling hyaluronic acid. *International Journal of Biological Macromolecules*, *15*(1), 3–10.

Oviatt, H. W., & Brant, D. A. (1994). Viscoelastic behavior of thermally treated aqueous xanthan solutions in the semidilute concentration regime. *Macromolecules*, *27*(9), 2402–2408.

Paoletti, S., Cesaro, A., & Delben, F. (1983). Thermally induced conformational transition of xanthan poly-electrolyte. *Carbohydrate Research*, *123*(1), 173–178.

Pelletier, E., Viebke, C., Meadows, J., & Williams, P. A. (2001). A rheological study of the order–disorder conformational transition of xanthan gum. *Biopolymers*, *59*(5), 339–346.

Rochefort, W. E., & Middleman, S. (1987). Rheology of xanthan gum: Salt, temperature, and strain effects in oscillatory and steady shear experiments. *Journal of Rheology*, *31*(4), 337–369.

Rodd, A. B., Dunstan, D. E., & Boger, D. V. (2000). Characterisation of xanthan gum solutions using dynamic light scattering and rheology. *Carbohydrate Polymers*, *42*(2), 159–174.

Ross-Murphy, S. B., Morris, V. J., & Morris, E. R. (1983). Molecular viscoelasticity of xanthan polysaccharide. *Faraday Symposia of the Chemical Society*, *18*, 115–129.

Sato, T., Norisuye, T., & Fujita, H. (1984). Double-stranded helix of xanthan: Dimensional and hydrodynamic properties in 0.1 M aqueous sodium chloride. *Macromolecules*, *17*(12), 2696–2700.

Song, K. W., Kim, Y. S., & Chang, G. S. (2006). Rheology of concentrated xanthan gum solutions: Steady shear flow behavior. *Fibers and Polymers*, *7*(2), 129–138.

Sworn. (2000). Xanthan gum. In G. O. Phillips, & P. A. Williams (Eds.), *Handbook of hydrocolloids* (pp. 103–116). Boca Raton: CRC Press.

Whitcomb, P. J., & Macosko, C. W. (1978). Rheology of xanthan gum. *Journal of Rheology*, *22*(5), 493–505.

Wyatt, N. B., & Liberatore, M. W. (2009). Rheology and viscosity scaling of the polyelectrolyte xanthan gum. *Journal of Applied Polymer Science*, *114*(6), 4076–4084.